https://doi.org/10.46813/2026-164-146

UDC 621.039.73

IRON-MODIFIED MAGNESIUM POTASSIUM PHOSPHATE CEMENT AS AN EFFECTIVE MATRIX FOR IMMOBILIZING RHENIUM, A CHEMICAL ANALOGUE OF TECHNETIUM

Sergii Sayenko, Volodymyr Shkuropatenko, Olexandr Pylypenko, Kostiantyn Lobach, Svitlana Karsim

National Science Center "Kharkiv Institute of Physics and Technology", Kharkiv, Ukraine

E-mail: shkuropatenko@kipt.kharkov.ua

The immobilization of non-radioactive Re, a chemical analogue of ^{99}Tc, in magnesium-potassium phosphate cement (MKPC)-based matrices was studied, as well as the possibility of enhancing their functional properties by introducing iron-containing additives: Fe_2O_3, Fe_3O_4, Fe, FeS, and ground blast furnace slag. The efficiency of the MKPC matrices was assessed based on the results of strength tests, aqueous leaching tests, and comprehensive materials characterization using X-ray diffraction, Raman spectroscopy, and scanning electron microscopy. The degree of Re(VII) reduction to the more stable valence form Re(IV) in the presence of iron-containing materials was determined using X-ray absorption spectroscopy. The results showed that the introduction of iron-containing additives into the initial powder mixture (MKPC + 5 wt.% Re_2O_7) has a positive effect on the compressive strength and water resistance of the resulting solid forms. High strength (49.6 MPa) and chemical resistance (leaching index 9.31) were demonstrated by MKPC samples with the addition of 10 wt.% ground blast furnace slag, which is due to the formation of a denser microstructure and high reducing properties of the slag.

INTRODUCTION

Technetium-99 (^{99}Tc), a β-emitter with a half-life of ~$2.13 \cdot 10^5$ years, is produced with a high yield (~6%) during the fission of ^{235}U and ^{239}Pu. Approximately 1 kg of ^{99}Tc is generated per ton of spent nuclear fuel. The immobilization of ^{99}Tc is one of the most challenging tasks in radioactive waste management due to its specific chemical and radiological properties. The migration of Tc in the environment is largely controlled by redox conditions, as it can exist in multiple oxidation states. Under oxidizing conditions, Tc(VII) predominates, whereas Tc(IV) is stable under reducing conditions. The high environmental risk associated with ^{99}Tc is due to its long half-life and the high mobility of Tc(VII), which exists as the pertechnetate anion TcO_4^- in oxidizing environments. Under reducing conditions, Tc(VII) is converted to Tc(IV), forming hydrated technetium dioxide $TcO_2 \cdot nH_2O$, which has low solubility and limited mobility [1]. Currently, considerable research focuses on the use of reactive iron-containing particles as effective reductants for Tc(VII). This approach is partly justified by the natural abundance of iron oxides, as well as the coupled reduction of technetium and iron observed under natural redox gradients [2].

To prevent technetium release into the environment, various strategies are being developed to immobilize its in stable waste forms that are resistant to dissolution and oxidation. Numerous waste forms have been proposed, including glass, ceramics, and cementitious materials [3, 4]. During vitrification, radioactive waste is mixed with glass frit (glass-forming components), after which the mixture is fed into a melting furnace operating at high temperatures of 1000…1250 °C. Retention of ^{99}Tc in glass under such conditions is challenging due to the high volatility of technetium compounds. Technetium oxides tend to volatilize at relatively low temperatures, as Tc_2O_7 boils at 311 °C, while TcO_2 sublimates between 900 and 1000 °C [3].

Magnesium potassium phosphate cement (MKPC), also known under the commercial name Ceramicrete, has been developed and studied as a material for the low-temperature conditioning of various challenging nuclear wastes, including plutonium-contaminated ash, liquid salt wastes, and sludge from radioactive waste storage tanks at the Hanford site (USA) [5, 6]. MKPC has also been applied for the solidification of liquid wastes containing ^{99}Tc [7]. To convert technetium from the +7 oxidation state to the more stable +4 state, 2…3 wt.% $SnCl_2$ was added to the initial mixture as a reducing agent. To enhance the mechanical strength and integrity of the final material, 38 wt.% fly ash was incorporated. As a result, the obtained waste forms exhibited a compressive strength of about 30 MPa and demonstrated high stability in aqueous environments.

According to [8], Ceramicrete phosphate cement modified with the addition of goethite (α-FeO(OH)) was synthesized and tested for the immobilization of residual wastes from tank C-202 at the Hanford site containing ^{99}Tc. Leaching tests in aqueous media confirmed the effectiveness of the proposed treatment: the fraction of released technetium decreased to 5.8…6.3%, compared to ~29% for untreated waste. However, the long-term stability of technetium-bearing phases immobilized in the presence of iron and its compounds remains insufficiently understood and requires further comprehensive investigation. In many studies, rhenium (Re) is used as a non-radioactive surrogate for ^{99}Tc, as their ionic species exhibit similar ionic radii and comparable hydration energies [9].

This study investigated the use of iron-containing additives (Fe_2O_3, Fe_3O_4, Fe, FeS and blast furnace slag–BFS) to improve the mechanical strength, integrity and

water resistance of Re-containing MKPC matrix. The choice of additives was driven by both the need to improve the characteristics of the matrix and the ability of iron compounds, also present in BFS, to effectively stabilize ^{99}Tc in nuclear waste, reducing it from an oxidation state of +7 to +4. X-ray absorption spectroscopy was employed to determine the average oxidation state of Re in MKPC samples. X-ray diffraction (XRD), Raman spectroscopy, and scanning electron microscopy (SEM) were used to characterize the MKPC material and to identify phase and structural changes following its interaction with incorporated rhenium in the form of Re_2O_7.

1. MATERIALS AND METHODS

Magnesium potassium phosphate cement is produced via a chemical reaction that forms magnesium potassium phosphate hexahydrate, $MgKPO_4 \cdot 6H_2O$, also named K-struvite. This process occurs through the interaction of magnesium oxide (MgO) with potassium dihydrogen phosphate (KH_2PO_4) in the presence of water, according to the following equation:

$$MgO + KH_2PO_4 + 5\ H_2O \rightarrow MgKPO_4 \cdot 6H_2O.$$

For MKPC synthesis, technical-grade potassium dihydrogen phosphate and magnesium oxide were used. MgO was thermally treated at 1200 °C for 2 h in air to reduce its reactivity. Boric acid (H_3BO_3) was added as a setting retarder. In the preparation of MKPC-based matrices, the following iron-containing modifying powders were used: hematite (Fe_2O_3), magnetite (Fe_3O_4), metallic iron (Fe), iron sulfide (FeS), and blast furnace slag, with the following chemical composition: CaO (25…40 wt.%), SiO_2 (30…40 wt.%), Al_2O_3 (10…20 wt.%), MgO (1…5 wt.%), and FeO (1…2 wt.%). The purity grades and suppliers of the raw materials are listed in Table 1.

Table 1

Characteristics of the raw materials

Components	Purity	Suppliers
Magnesium oxide (MgO)	≥98%	Carl Roth®
Potassium dihydrogen Phosphate (KH_2PO_4)	≥98%	Carl Roth®
Boric acid (H_3BO_3)	>99%	PENTA Chemicals Unlimited®
Rhenium oxide (Re_2O_7)	≥99.9	SIGMA-ALDRICH
Hematite (Fe_2O_3)	>99%	SIGMA-ALDRICH
Magnetite (Fe_3O_4)	97%	ThermoFisher®
Metallic iron (Fe)	>99%	SIGMA-ALDRICH
Iron sulfide (FeS)	97%	LACHEMA N.P.BRNO, Czech Republic
Blast furnace slag	–	Moravia Steel, Trinec, Czech Republic

For the preparation of MKPC, a molar ratio (M/P=2.25) of magnesium oxide to phosphate KH_2PO_4 and a water-to-cement mass ratio (W/C=0.5) were used, as previously proposed for MKPC waste forms in the immobilization of minor actinides [10]. Re_2O_7 and modifying additives were incorporated into the mixture at 5 wt.% and 10 wt.%, respectively, relative to the mass of the reactive binder components (MgO and KH_2PO_4) (Table 2). The dry powder components (MgO, KH_2PO_4, Re_2O_7, and the iron-containing additive) were mixed according to the formulation in a laboratory mill (ALPINE Augsburg, Germany) for 10 min. Subsequently, H_3BO_3 (5 wt.% relative to MgO and KH_2PO_4) was dissolved in deionized water. The dry mixture was then added to this solution, mechanically stirred for 3 min, and cast into plastic molds (3×3×3 cm). The samples were demolded after 24 h and subsequently cured in air at (22.5±2.5) °C.

Table 2

Formulations of powder compositions for obtaining MKPC matrices

Formulations	Dry mix proportions, wt.%						
	$MgO + KH_2PO_4$	Re_2O_7	Fe_2O_3	Fe_3O_4	Fe	FeS	BFS
M	100	–	–	–	–	–	–
M-Re	95	5	–	–	–	–	–
M-Re-Fe_2O_3	85	5	10	–	–	–	–
M-Re-Fe_3O_4	85	5	–	10	–	–	–
M-Re-Fe	85	5	–	–	10	–	–
M-Re-FeS	85	5	–	–	–	10	–
M-Re-BFS	85	5	–	–	–	–	10

The compressive strength of MKPC samples after 1, 7, and 28 days of curing was evaluated by measuring compressive strength using a universal testing machine (MEGA II-600 DMI-S, Germany) at a loading rate of 0.25 MPa/s. The average compressive strength was determined as the mean value of three specimens. The phase composition of the obtained materials was analyzed using Bragg–Brentano powder X-ray diffraction. Diffraction patterns were recorded using a PANalytical X'Pert PRO diffractometer equipped with a conventional X-ray tube (Cu K_α radiation, 40 kV, 30 mA, line focus) and a PIXcel linear position-sensitive detector with an anti-scatter screen. Qualitative analysis was performed using the HighScore Plus software package (Malvern PANalytical, version 5.3.1) in conjunction with the PDF-5+ database [11]. Quantitative analysis of the

experimental data was carried out using the Rietveld refinement method [12].

To determine the average oxidation state of Re in MKPC samples and to investigate the local atomic environment around the absorbing Re atoms, X-ray absorption spectroscopy (XAS) was employed. X-ray absorption near-edge structure (XANES) spectra at the Re L_3-edge (10.534 eV) were collected in transmission mode, with each spectrum averaged over three measurements. A metallic Re foil was measured simultaneously as a reference. The acquired spectra were processed using the Athena software from the Demeter package (version 0.9.26) [13], based on the IFEFFIT algorithm, for energy alignment with the reference foil and normalization.

The fracture surface morphology of the samples was analyzed using scanning electron microscopy coupled with energy-dispersive X-ray spectroscopy (EDS) on a JSM-6510 microscope (JEOL Ltd., Japan). Raman spectroscopy was performed using a DXR Raman spectrometer (Thermo Fisher Scientific Inc., USA). The spectral range used for the characterization of MKPC materials was 0…3600 cm^{-1}.

The leaching behavior of the MKPC matrix was investigated using the American National Standard ANSI/ANS-16.1 test method [14]. Leaching tests of the prepared MKPC samples were conducted in deionized water over five intervals at 1, 4, 14, 28, and 43 days (total duration of 90 days) in plastic containers at room temperature. The concentrations of Re released from the samples were determined using inductively coupled plasma atomic emission spectroscopy (ICP-AES, iCAP 6300 Duo, Thermo Scientific Corporation).

2. RESULTS AND DISCUSSION

2.1. MECHANICAL STRENGTH

Mechanical strength testing of MKPC samples containing Re_2O_7 and various iron-bearing additives was performed after 1, 7, and 28 days of curing, and the results are presented in Fig. 1. The compressive strength of MKPC without additives was 37.2 MPa. The addition of rhenium oxide led to a decrease in strength for the MKP–Re specimen (34 MPa) after 28 days of curing. The average compressive strength values of MKPC with iron-containing additives increased compared to M–Re without additives at all curing stages. The maximum compressive strength, 49.6 MPa, was achieved for the M–Re–BFS composition. The addition of 10 wt.% blast furnace slag increased the strength by 46 % compared to MKPC without additives.

Different countries establish different Waste Acceptance Criteria (WAC), specifically the minimum compressive strength required for cement waste forms intended for disposal at radioactive waste repositories. For example, the minimum compressive strength is 3.45 MPa in the United States, 5 MPa in Ukraine, 8 MPa in France, and 10 MPa in Italy. The obtained compressive strength values of MKPC samples exceed the generally accepted WAC requirements for cementitious waste matrices.

Our conclusions that BFS additives contribute to achieving high mechanical strength of MKPC were confirmed by other researchers. Previously, Gardner et al. [15] investigated the structure and properties of magnesium potassium phosphate cements containing 50 wt.% ground granulated blast furnace slag or fly ash (FA).

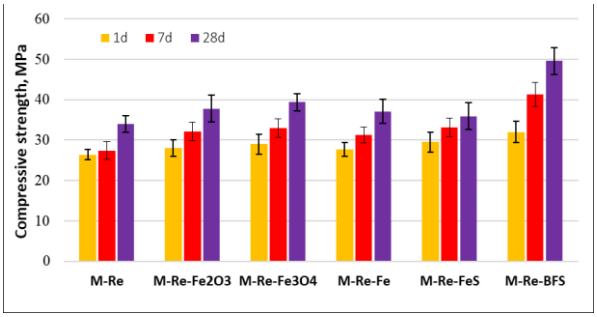


Fig. 1. Compressive strength of MKPC samples with Re_2O_7 and additives of Fe_2O_3, Fe_3O_4, Fe, FeS, BFS

A significant increase in compressive strength was observed for MKPC with slag compared to MKPC without additives, whereas MKPC with fly ash achieved strength values comparable to those of additive-free MKPC. Sayenko et al. [16] reported a 44% increase in compressive strength for MKPC with blast furnace slag compared to MKPC with fly ash after 28 days of curing. Liu et al. [17] noted that slag addition can improve the early mechanical properties of MKPC due to both the physical filler effect and chemical interactions.

One of the common explanations for the increase in compressive strength of MKPC with the addition of BFS or FA is related to the chemical composition of these additives. BFS and FA are rich in reactive forms of SiO_2 and Al_2O_3, which are present in amorphous or poorly crystalline phases, making them available for dissolution in the mildly alkaline saline environment of MKPC. As a result of silicon and aluminum reactions, additional aluminosilicate phases are formed [15]. These phases act as “cementing bridges” within pores and between crystals of the main product – K-struvite thereby reducing defects and increasing structural density and, consequently, the strength of the material. However, the exact type and structure of these aluminosilicates remain undefined. The structure is likely an oxygen tetrahedral framework similar to that of geopolymers, whose mechanical properties are generally superior to those of K-struvite [18].

It is well known that as the hydration reaction between MgO and phosphate progresses, the pH of the system gradually increases. According to Xu et al. [19], during MKPC hydration, a decrease in pH occurs only at the initial stage (approximately 2 min), after which it gradually increases to about 9.0, with a brief drop to 8.4 between 22 and 35 min. Subsequently, from 35 min to 24 h, the pH rises to 11.8, indicating that MKPC synthesis predominantly occurs under alkaline conditions. Thus, the chemical environment transitions from initially acidic to alkaline, where a geopolymer-like structure may form in the presence of significant amounts of silicon- and aluminum-containing additives. Therefore, silicon and aluminum likely interact to form Si-Al-O tetrahedral networks similar to geopolymeric structures. The formation of such complexes promotes an increase in hydration products, which in turn enhances the overall

density and improves the mechanical properties of MKPC [20].

In contrast to BFS, the additives Fe_2O_3, Fe_3O_4, Fe, and FeS only slightly increase the compressive strength of MKPC (see Fig. 1). According to [21], the addition of Fe_2O_3 and Fe_3O_4 to the magnesium potassium phosphate cement system does not lead to the formation of new crystalline phases and does not involve chemical interactions, acting instead as inert fillers. Evidently, Fe and FeS additives also influence the strength of MKPC only physically, functioning as fillers.

2.2. ANALYTICAL RESEARCH

Fig. 2 presents the X-ray diffraction pattern of MKPC containing 5 % Re_2O_7 (M-Re). The addition of 5% Re_2O_7 leads to the formation of potassium perrhenate ($KReO_4$), with a fraction of 6.87 %. $KReO_4$ is identified alongside K-struvite (76.71%) and residual unreacted MgO (16.42%). The presence of potassium perrhenate salt in the MCPC matrix explains the observed decrease in the compressive strength of the M–Re sample compared to MKPC without the addition of Re_2O_7.

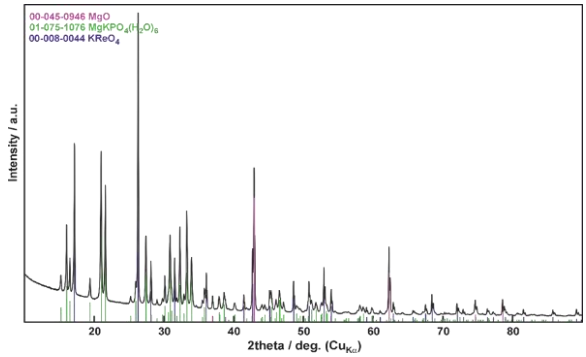


Fig. 2. Diffractogram of MKPC samples with the addition of 5% Re_2O_7

The Raman spectra of MKPC without additives, MKPC with 5% Re_2O_7 (M-Re), and Re_2O_7 powder are shown in Fig. 3. In the spectrum of M–Re, distinct bands are observed at 228, 426, 462, 562, and 943 cm^{-1}, which are characteristic of K-struvite [22], as well as a signal around 295 cm^{-1} corresponding to MgO [23]. All these peaks are also present in the spectrum of additive-free MKPC. Thus, the obtained data are consistent with the XRD results (see Fig. 2) and confirm the presence of the main phase in MKPC – K-struvite, as well as residual MgO. Additional bands in the M–Re spectrum at 50, 333, 347, 892, 919, and 959 cm^{-1} correspond to potassium perrhenate $KReO_4$, the presence of which is also confirmed by X-ray diffraction analysis.

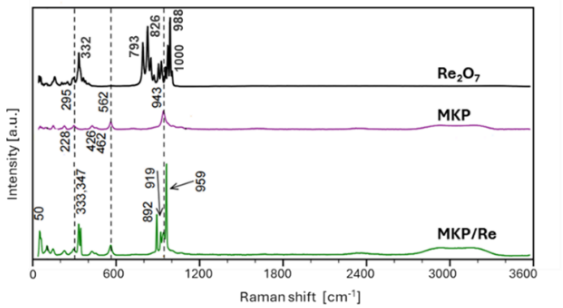


Fig. 3. Raman spectra of M, M-Re sample and Re_2O_7 powder

In [24], characteristic peaks for $KReO_4$ are reported at 49, 335, 893, 910, and 969 cm^{-1}. As shown in Table 3, the $KReO_4$ peaks identified in the M–Re composition slightly differ from the literature values, particularly due to the appearance of a band at 347 cm^{-1} and a shift of approximately 10 cm^{-1} for the peaks at 919 and 959 cm^{-1}. The Raman spectrum of Re_2O_7 powder exhibits peaks at 158, 296, 332, 364, 793, 826, 849, 873, 905, 925, 956, 972, 988, and 1000 cm^{-1}, which are characteristic of this compound [25]. The absence of these bands in the M–Re spectrum indicates the complete dissolution of Re_2O_7 and its subsequent reaction leading to the formation of $KReO_4$.

Table 3

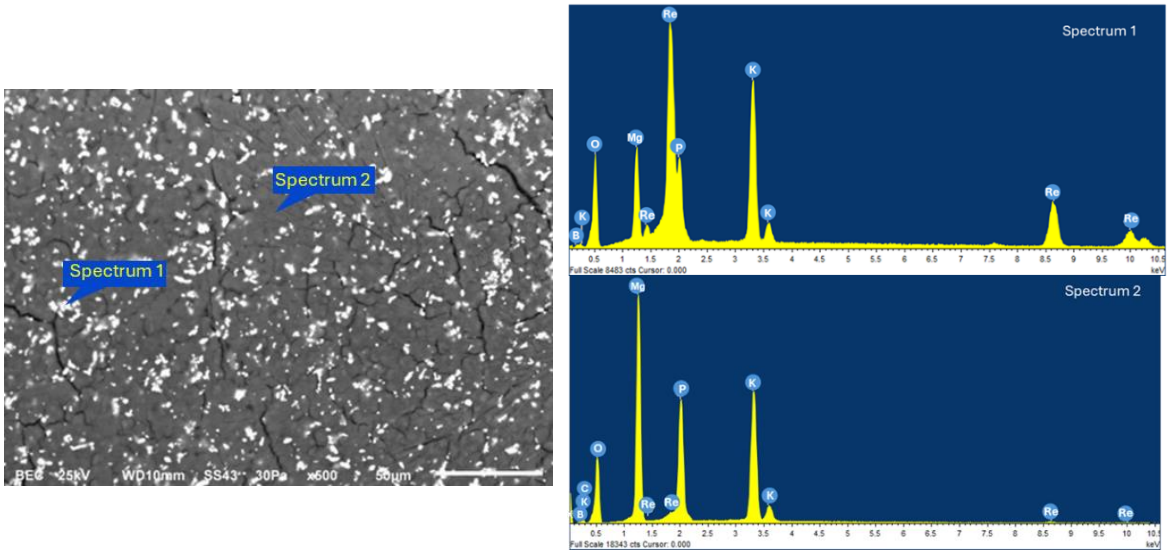
Raman spectral data for struvite and $KReO_4$

Raman peaks of struvite, cm^{-1}		Raman peaks of $KReO_4$, cm^{-1}	
observed	reference [22]	observed	reference [25]
–	–	50	49
228	228.5	–	–
–	–	333	335
–	–	347	–
426	427.5	–	–
462	462.8	–	–
562	564.1	–	–
–	–	892	893
–	–	919	910
943	941.8	–	–
–	–	959	969

Fracture surfaces of MKPC samples containing 5% Re_2O_7 after compressive strength testing were analyzed using scanning electron microscopy. A significant number of bright particles surrounded by a dark matrix were observed (Fig. 4,a).

EDS analysis of the bright particles shows pronounced intense peaks of Re, K, and O, indicating that these particles consist of potassium perrhenate, $KReO_4$ (Fig. 4,b). The potassium perrhenate particles, with sizes not exceeding 5 μm, exhibit a broad particle size distribution, are fairly uniformly distributed within the matrix, and show a tendency to form aggregates. The EDS spectrum of the dark material clearly displays distinct peaks of magnesium, potassium, phosphorus, and oxygen, indicating that this material is primarily composed of magnesium potassium phosphate cement.

A comprehensive study of the MKPC-based matrix using X-ray diffraction, Raman spectroscopy, and SEM/EDS analysis showed that the incorporation of 5 wt.% powdered Re_2O_7 results in the formation of potassium perrhenate $KReO_4$, in addition to K-struvite and unreacted MgO, within the hardened matrix. SEM data indicate that $KReO_4$ is present as particles of various sizes embedded within the structure of the MKPC matrix.



a *b*

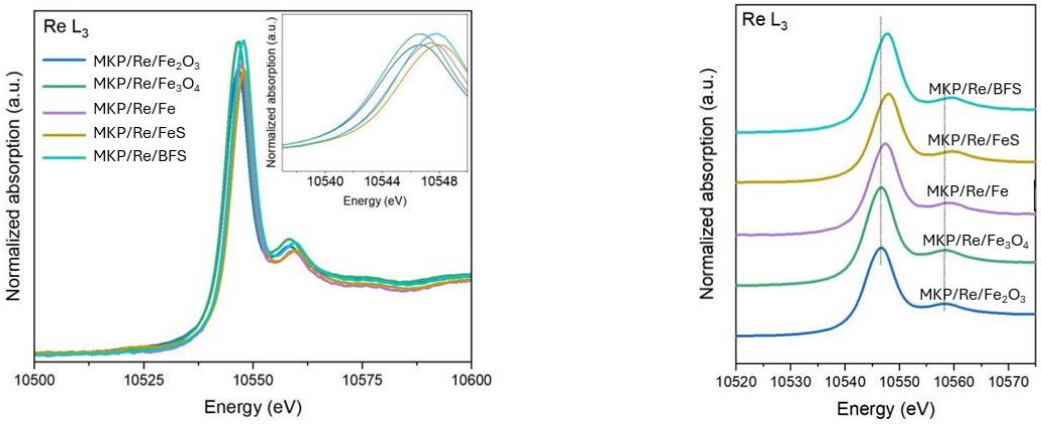
Fig. 4. SEM images of the M-Re sample: a – microstructure; b – EDS spectra of $KReO_4$ (Spectrum 1), and MKPC (Spectrum 2)

To determine the average oxidation state of rhenium in the MKPC matrix, X-ray absorption spectroscopy was applied. The Re L_3 edge XANES spectra are shown in Fig. 5, and the edge positions are presented in Table 4. The obtained spectra indicate that rhenium is predominantly present in the high oxidation state Re(VII), although a certain fraction of reduced species is also present. The absorption edge for Re in M-Re-Fe_2O_3 is 10543.87 eV, whereas for M-Re-FeS it is shifted to 10545.27 eV, corresponding to a difference of 1.4 eV. As is well known [26], the position of the L_3-edge is an indicator of the oxidation state: with decreasing valence, the intensity of the white line decreases and the edge position shifts.

Table 4

Position of Re L_3 edge peaks in XANES spectra

Specimen	Edge Energy (E_0)
M-Re-Fe_2O_3	10543.9
M-Re-Fe_3O_4	10544.0
M-Re-Fe	10544.7
M-Re-BFS	10545.0
M-Re-FeS	10545.3



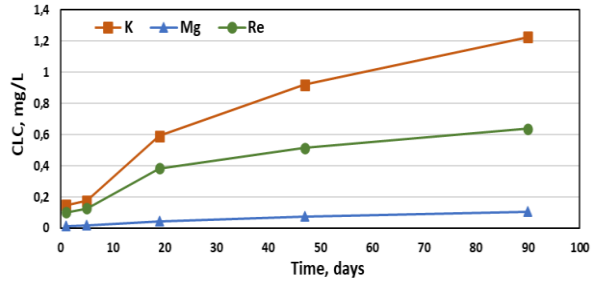
a *b*

Fig. 5. XANES study results: a – Re L_3 XANES spectra in MKPC with Fe_2O_3, Fe_3O_4, Fe, FeS, and BFS additives; b – expanded image of the Re L_3 absorption edge highlighting systematic shifts in the white line position as a function of dopant

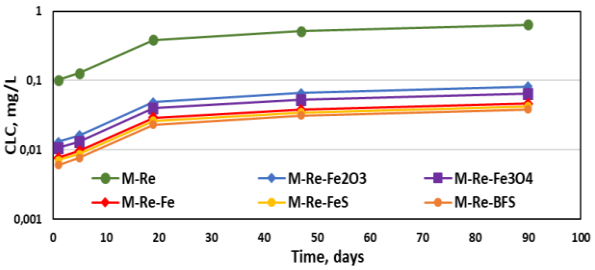
The results obtained indicate that rhenium is mainly in the +7 oxidation state; however, partial reduction leads to the presence of a mixture of valence states, likely including Re(VI) and/or Re(IV) alongside the dominant Re(VII). The general trend of the studied MKPC-based materials in terms of the degree of rhenium reduction is as follows: the most reduced is M-Re-FeS, followed by M-Re-BFS, M-Re-Fe, M-Re-Fe_3O_4, and the least reduced is M-Re-Fe_2O_3.

2.3. LEACHING TEST

Leaching test data for MKPC samples, obtained in accordance with the ANSI/ANS-16.1 standard, are presented as cumulative leached concentrations (CLC) of the main matrix elements (Mg, K) and Re (Fig. 6). The effective diffusion coefficient (D_e) and leachability index (LI) were also calculated using the equations provided in the ANSI/ANS-16.1 standard [14]. Fig. 6,a shows the CLC values for potassium, rhenium, and magnesium for the M-Re sample, which after 90 days reached $1.23 \cdot 10^{-6}$, $0.64 \cdot 10^{-6}$, and $0.11 \cdot 10^{-6}$ g/l, respectively. The results indicate that potassium is leached from the MKPC matrix to the greatest extent compared to rhenium and magnesium, following the order: K>Re>Mg. The calculated effective diffusion coefficient and leachability index are $1.14 \cdot 10^{-8}$ cm^2/s and 8.20 for Re, $3.70 \cdot 10^{-9}$ cm^2/s and 8.57 for K, and $1.70 \cdot 10^{-11}$ cm^2/s and 10.90 for Mg, respectively.



a



b

Fig. 6. Cumulative leaching concentrations: a – K, Re and Mg; b – Re of MKPC samples with additives of Fe_2O_3, Fe_3O_4, Fe, FeS, and BFS

Comparison of the cumulative leached concentrations of Re for MKPC matrices without additives and with additives shows that the incorporation of iron-containing additives significantly reduces this parameter. One possible reason is the formation of locally reducing conditions for Re(VII), caused by the presence of iron ions in the fillers, which is consistent with the XANES results (see Fig. 5, Table 4). Among the iron-containing additives, the highest Re leaching is observed for the sample with Fe_2O_3, with the substitution of additives by Fe_3O_4, Fe, FeS, and BFS, the leaching intensity gradually decreases, reaching minimum values when BFS is used.

The effective diffusion coefficients of Re for M-Re, M-Re-Fe_2O_3, M-Re-Fe_3O_4, M-Re-Fe, M-Re-FeS, and M-Re-BFS, as well as the corresponding leachability indices, were calculated and are presented in Fig. 7. The obtained results show that D_e values range from the highest value of $1.14 \cdot 10^{-8}$ cm^2/s for MKPC without iron-containing additives to the lowest value of $8.94 \cdot 10^{-10}$ cm^2/s when BFS is added. The incorporation of iron-containing additives increases the leachability index compared to the initial MKPC: the increase is 5.1% for M-Re-Fe_2O_3, 8.2% for M-Re-Fe_3O_4, 11.3% for M-Re-Fe, 12.9% for M-Re-FeS, and 13.5% for M-Re-BFS. The highest LI value (9.31) is achieved with the addition of 10% BFS.

All obtained LI values exceed the acceptance criterion for radioactive waste forms intended for disposal at controlled facilities (LI≥6.0 [27]). Since a higher LI and lower D_e correspond to better contaminant retention, this indicates that Re is most effectively immobilized in the magnesium potassium phosphate cement matrix containing BFS compared to the other studied MKPC systems.

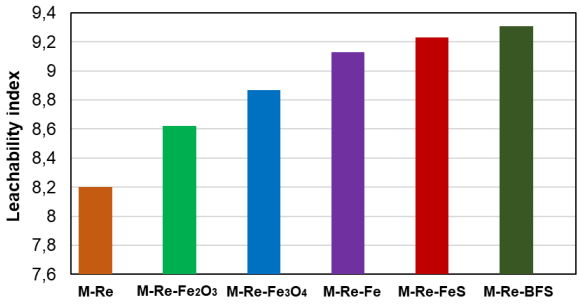


Fig. 7. Leachability indices Re

Blast furnace slag contains iron ions and sulfide components capable of acting as strong reducing agents for ^{99}Tc, thereby enhancing its immobilization efficiency in the cement matrix. After partial dissolution in the pore solution, both Fe(II) and S(II) exhibit high reactivity and can effectively reduce ^{99}Tc(VII) to the more stable and sparingly soluble Tc(IV) [28]. In this study, XANES confirmed the more pronounced reducing properties of both FeS and BFS. It was shown that FeS provides the highest degree of reduction of Re(VII) to Re(IV) among all the studied fillers, while BFS ranks second in terms of reducing activity. In addition, the use of BFS results in the highest compressive strength of MKPC (see Fig. 1), indicating the formation of a denser and more homogeneous microstructure compared to samples modified with Fe_2O_3, Fe_3O_4, Fe, and FeS, and, consequently, enhanced resistance of the material in an aqueous environment.

As a result of this study, it was found that the MKPC matrix containing BFS exhibits the highest strength and the greatest ability to retain Re (and therefore Tc) in an aqueous environment, due to its denser structure and the high reducing capacity of blast furnace slag.

CONCLUSIONS

In this study, the following results were obtained to evaluate the effectiveness of using magnesium potassium phosphate cement modified with iron-containing additives as a matrix for the immobilization of non-radioactive rhenium, a chemical analogue of ^{99}Tc.

1. The incorporation of iron-containing additives into the initial powder mixture (MKPC + 5 wt.% Re_2O_7) had a positive effect on the mechanical strength of the resulting solid forms. The compressive strength of samples modified with 10 wt.% Fe_2O_3, Fe_3O_4, Fe, FeS, and BFS after 28 days of curing was 37.8, 39.4, 37.1, 35.9, and 49.6 MPa, respectively. These strength values exceed the WAC requirement (5 MPa) for the acceptance

of cemented waste forms at radioactive waste disposal facilities.

2. The phase composition of MKPC changes after the addition of 5 wt.% powdered Re_2O_7: in addition to the main phases – K-struvite (77%) and periclase (16%) a new compound, potassium perrhenate ($KReO_4$), is formed in the material, accounting for approximately 7%. SEM analysis revealed that $KReO_4$ particles exhibit a wide size distribution (up to 5 μm) and are incorporated into the MKPC matrix, thereby limiting the contact of Re with the external environment.

3. The oxidation state of Re in the presence of reducing additives, such as Fe_2O_3, Fe_3O_4, Fe, FeS, and BFS, was investigated. XANES data indicate that Re is predominantly retained in the Re(VII) form. At the same time, the spectral features suggest partial reduction, manifested by the presence of mixed valence states – most likely Re(VI) and/or Re(IV) alongside the dominant Re(VII). The overall trend in the reducing capacity of the fillers follows the order: FeS (highest reduction degree), BFS, Fe, Fe_3O_4, Fe_2O_3 (lowest).

4. The addition of iron-containing additives to MKPC improves its water resistance, as confirmed by leaching tests conducted in accordance with the ANSI/ANS-16.1 standard. The maximum leachability index for Re in the MKPC sample with the addition of BFS reached 9.31, exceeding the target value (LI>6). This indicates the high efficiency of MKPC matrices containing BFS for ^{99}Tc encapsulation.

ACKNOWLEDGEMENTS

The authors express their sincere gratitude to their Czech colleagues (Nuclear research institute – UJV Rez) for their support, cooperation and the opportunity to conduct this research. Special thanks are extended to Dr. P. Večerník and Dr. V. Kašpar for discussions related to the preparation of MKPC samples and strength testing, Dr. P. Ecorchard for SEM and Raman spectroscopy, and Dr. P. Bezdicka for XRD analysis.

REFERENCES

1. A.H. Meena, Y. Arai. Environmental geochemistry of technetium // *Environ. Chem. Lett*. 2017, v. 15(2), p. 241-263; https://doi.org/10.1007/s10311-017-0605-7

2. D.M. Fan, R.P. Anitori, B.M. Tebo, P.G. Tratnyek, J.S.L. Pacheco, R.K. Kukkadapu, M.H. Engelhard, M.E. Bowden, L. Kovarik, B.W. Arey. Reductive sequestration of pertechnetate ($^{99}TcO_4^-$) by nano zerovalent iron (nZVI) transformed by abiotic sulfide // *Environ. Sci. Technol.* 2013, v. 47, p. 5302-5310; https://pubs.acs.org/doi/10.1021/es304829z

3. B.K. Singh, N.S. Mahzan, N.S.A. Rashid, S.A. Isa, M.A. Hafeez, S. Saslow, G. Wang, C. Mo, W. Um. Design and Application of Materials for Sequestration and Immobilization of ^{99}Tc // *Environ. Sci. Technol.* 2023, v. 57, N 17, p. 6776-6798; https://doi.org/10.1021/acs.est.3c00129

4. B.K. Singh, J. Kim, D. Pak, K. Kim, W. Um. Technetium (Tc)/Rhenium (Re) solubility and leaching behavior from waste forms: An overview // *Front. Nucl. Eng*. *Sec. Radioactive Waste Management*. 2023, 1-2022; https://doi.org/10.3389/fnuen.2022.1112080

5. A.S. Wagh, R. Strain, S.Y. Jeong, D. Reed, T. Krause, D. Singh. Stabilization of Rocky Flats Pucontaminated ash within chemically bonded phosphate ceramics // *Journal of Nuclear Materials.* 1999, v. 265, p. 295-307; https://doi.org/10.1016/S0022-3115(98)00650-3

6. S.Yu. Sayenko, V.A. Shkuropatenko, O.V. Pylypenko, S.O. Karsim, A.V. Zykova, D.V. Kutnii, Arun S. Wagh. Radioactive Waste Immobilization of Hanford Sludge in Magnesium Potassium Phosphate Ceramic Forms // *Progress in Nuclear Energy.* 2022, v. 152, p. 104315; https://doi.org/10.1016/j.pnucene.2022.104315

7. D. Singh, V. Mandalika, S. Parulekar, A. Wagh. Magnesium potassium phosphate ceramic for ^{99}Tc immobilization // *J. Nucl. Mater*. 2006, v. 348, p. 272-282; https://doi.org/10.1016/j.jnucmat.2005.09.026

8. K. Cantrell, W. Um, B. Williams, M. Bowden, B. Gartman, W. Lukens, E. Buck, E. Mausolf. Chemical stabilization of Hanford tank residual waste // *J. Nucl. Mater.* 2014, v. 446, p. 246-256; https://dx.doi.org/10.1016/j.jnucmat.2013.10.060

9. D. Kim, A.A. Kruger. Volatile species of technetium and rhenium during waste vitrification // *J. Non-Cryst. Solids.* 2018, v. 481, p. 41-50; https://doi.org/10.1016/j.jnoncrysol.2017.10.013

10. H.-C.Z. Loye, P. Vecernik, M. Kiselova, V. Kašpar, H. Korenkova, V. Miller, P. Bezdicka, J. Šubrt, N. Murafa, V. Shkuropatenko, S. Sayenko. Investigation of Magnesium-Potassium Phosphates as Potential Nuclear Waste Form for the Immobilization of Minor Actinides // *Inorganics.* 2024, v. 12, p. 311; https://doi.org/10.3390/inorganics12120311

11. S. Kabekkodu, A. Dosen, T. Blanton. PDF-5+: A comprehensive Powder Diffraction File™ for materials characterization // *Powder Diffr.* 2024, v. 39, p. 47-59; https://doi.org/10.1017/S0885715624000150

12. H.M. Rietveld. A profile refinement method for nuclear and magnetic structures // *J. Appl. Crystallogr.* 1969, v. 2, p. 65-71; https://doi.org/10.1107/S0021889869006558

13. B. Ravel, M. Newville. ATHENA, ARTEMIS, HEPHAESTUS: Data analysis for X-ray absorption spectroscopy using IFEFFIT // *J. Synchrotron Radiat.* 2005, v. 12, p. 537-541; https://doi.org/10.1107/S0909049505012719

14. ANSI/ANS-16.1; Measurement of Leachability in Solidified Low-Level Radioactive Waste by the Short-Term Procedure – An American National Standard. American Nuclear Society: Westmont, IL, USA, 2019.

15. L. Gardner, S. Bernal, S. Walling, C. Corkhill, J. Provis, N. Hyatt. Characterisation of magnesium potassium phosphate cements blended with fly ash and ground granulated blast furnace slag // *Cem. Concr. Res.* 2015, v. 74, p. 78-87; https://dx.doi.org/10.1016/j.cemconres.2015.01.015

16. S. Sayenko, V. Shkuropatenko, O. Pylypenko, H. Kholomieiev, S. Karsim, A. Zykova. Production and Properties of Magnesium Potassium Phosphate Cements Containing Ash and Metallurgical Slag Additives for RadioactiveWaste Immobilization // *Nucl. Rad. Saf.* 2023, v. 2, p. 30-43; https://doi.org/10.32918/nrs.2023.2(98).03

17. Kuisheng Liu, Shanliang Ma, Zengqi Zhang and Fanghui Han. Hydration and Properties of Magnesium Potassium Phosphate Cement Modified by Granulated

Blast-Furnace Slag: Influence of Fineness // *Materials.* 2022, v. 15, p. 918; https://doi.org/10.3390/ma15030918

18. Sam A. Walling and John L. Provis. Magnesia-Based Cements: A Journey of 150 Years, and Cements for the Future? // *Chem. Rev.* 2016, v. 116, p. 4170-4204; https://doi.org/10.1021/acs.chemrev.5b00463

19. Biwan Xu, Barbara Lothenbach, Andreas Leemann, Frank Winnefeld. Reaction mechanism of magnesium potassium phosphate cement with high magnesium-to-phosphate ratio // *Cement and Concrete Research.* 2018, v. 108, p. 140-151; https://doi.org/10.1016/j.cemconres.2018.03.013

20. Qiushi Zhang, Xing Cao, Rui Ma, Shichang Sun, Lin Fang, Junhao Lin, Juan Luo. Solid waste-based magnesium phosphate cements: Preparation, performance and solidification/stabilization mechanism // *Construction and Building Materials.* 2021, v. 297, p.1237; https://doi.org/10.1016/j.conbuildmat.2021.123761

21. S. Sayenko, V. Shkuropatenko, P. Vecernik, V. Kašpar, M. Kiselova, S. Karsim, I. Kolodiy, P. Mateychenko, K. Lobach, A. Zykova. The effect of Fe_2O_3 and Fe_2O_3/Fe_3O_4 additives on the hydration, structure and strength of magnesium potassium phosphate cement for the immobilization radioactive wastes // *Problems of Atomic Science and Technology*. 2025, N 2(156), p. 61-70; https://doi.org/10.46813/2025-156-061

22. Ray L. Frost, Matt L. Weier, Wayde N. Martens, Dermot A. Henry and Stuart J. Mills. Raman spectroscopy of newberyite, hannayite and struvite // *Spectrochimica Acta.* 2005, v. 62(1), p. 181-188; https://dx.doi.org/10.1016/J.SAA.2004.12.024

23. K. Ishikawa, N. Fujima, and H. Komura. First-order Raman scattering in MgO microcrystals // *J. Appl. Phys.* 1985, v. 57, p. 973; https://dx.doi.org/10.1063/1.334701

24. Miao-Miao Li, Jing-Wen Cao, Xiao-Ling Qin, Xiao-Yan Liu, Xiao-Qing Yuan, Xiao-Tong Dong, Qing Guo, Yi Sun, and Peng Zhang. Theoretical Prediction of Rhenium Separation from Ammonium Perrhenate by Phonon-Photon Resonance Absorption // *ACS Omega.* 2022, v. 7, p. 5437-5441; https://doi.org/10.1021/acsomega.1c06744

25. R. Beattie and G.A. Ozin. Vibrational Spectrum of Gaseous, Liquid, and Solid Re_2O_7 // *J. Chem. SOC. (A).* 1969, p. 2615-2619; https://doi.org/10.1039/J19690002615

26. A. Tougerti, S. Cristol, E. Berrier, V. Briois, C. Fontaine, F. Villain, Y. Joly. XANES study of rhenium oxide compounds at the L_1 and L_3 absorption edges // *Physical Review B.* 2012, v. 85, p. 125136; https://doi.org/10.1103/PhysRevB.85.125136

27. Tech/Position. U.S. Nuclear Regulatory Commission, Technical Position on Waste Form. Washington DC, 20555 Revision 1. Appendix A-7. 1991; www.nrc.gov/docs/ML0037/ML003752851.pdf

28. Wooyong Um, Jung-Seok Yang, R. Jeffrey Serne, Joseph H. Westsik. Reductive capacity measurement of waste forms for secondary radioactive wastes // *Journal of Nuclear Materials.* 2015, v. 467, p. 251-259; https://dx.doi.org/10.1016/j.jnucmat.2015.09.045

Article received 06.07.2026

МОДИФІКОВАНИЙ ЗАЛІЗОМ МАГНІЄВО-КАЛІЄВИЙ ФОСФАТНИЙ ЦЕМЕНТ ЯК ЕФЕКТИВНА МАТРИЦЯ ДЛЯ ІММОБІЛІЗАЦІЇ РЕНІЮ, ХІМІЧНОГО АНАЛОГА ТЕХНЕЦІЮ

Сергій Саєнко, Володимир Шкуропатенко, Олександр Пилипенко, Костянтин Лобач, Світлана Карсім

Досліджено іммобілізацію нерадіоактивного Re, хімічного аналога ^{99}Tc, у матрицях на основі магнієво-калієвого фосфатного цементу (МКФЦ), а також можливість підвищення їхніх функціональних властивостей шляхом введення залізовмісних добавок: Fe_2O_3, Fe_3O_4, Fe, FeS та меленого доменного шлаку. Ефективність МКФЦ-матриць оцінювали за результатами випробувань на міцність, тестів на вилуговування у водному середовищі та комплексної матеріалознавчої характеристики методами рентгенівської дифракції, раманівської спектроскопії та скануючої електронної мікроскопії. Ступінь відновлення Re(VII) до більш стабільної валентної форми Re(IV) у присутності залізовмісних матеріалів визначали за допомогою рентгенівської абсорбційної спектроскопії. Отримані результати засвідчили, що введення залізовмісних добавок у вихідну порошкову суміш (МКФЦ+5 мас.% Re_2O_7) позитивно впливає на міцність на стиск та водостійкість сформованих твердих форм. Найвищі показники міцності (49,6 МПа) та хімічної стійкості (індекс вилуговування 9,31) продемонстрували зразки МКФЦ із добавкою 10 мас.% меленого доменного шлаку, що зумовлено формуванням щільнішої мікроструктури та високими відновлювальними властивостями шлаку.